

Experimental violation of a Bell-like inequality with optical vortex beams

B. Stoklasa,¹ L. Motka,¹ J. Rehacek,¹ Z. Hradil,¹ L. L. Sánchez-Soto,^{2,3} and G. S. Agarwal⁴

¹*Department of Optics, Palacký University, 17. listopadu 12, 771 46 Olomouc, Czech Republic*

²*Departamento de Óptica, Facultad de Física, Universidad Complutense, 28040 Madrid, Spain*

³*Max-Planck-Institut für die Physik des Lichts, Günther-Scharowsky-Straße 1, Bau 24, 91058 Erlangen, Germany*

⁴*Department of Physics, Oklahoma State University, Stillwater, Oklahoma 74078, USA*

Optical beams with topological singularities have a Schmidt decomposition. Hence, they display features typically associated with bipartite quantum systems; in particular, these classical beams can exhibit entanglement. This classical entanglement can be quantified by a Bell inequality formulated in terms of Wigner functions. We experimentally demonstrate the violation of this inequality for Laguerre-Gauss (LG) beams and confirm that the violation increases with increasing orbital angular momentum. Our measurements yield negativity of the Wigner function at the origin for LG_{10} beams, whereas for LG_{20} we always get a positive value.

PACS numbers: 03.65.Ud, 42.50.Tx, 03.67.Bg, 42.50.Dv

I. INTRODUCTION

Entanglement is usually presented as one of the weirdest features of quantum theory that depart strongly from our common sense [1]. Since the seminal work of Einstein, Podolsky, and Rosen (EPR) [2], countless discussions on this subject have popped up [3].

A major step in the right direction is due to Bell [4], who formulated the EPR dilemma in terms of an inequality which naturally led to a falsifiable prediction. Actually, it is common to use an alternative formulation, derived by Clauser, Horne, Shimony and Holt (CHSH) [5], which is better suited for realistic experiments.

The main stream of research [6, 7] settled the main concepts of this topic in the realm of quantum physics. However, in recent years a general consensus has been reached on the fact that entanglement is not necessarily a signature of the quantumness of a system. Actually, as aptly remarked in RefE. [8], one should distinguish between two types of entanglement: between spatially separated systems (inter-system entanglement) and between different degrees of freedom of a single system (intra-system entanglement). Inter-system entanglement occurs only in truly quantum systems and may yield to nonlocal statistical correlations. Conversely, intra-system entanglement may also appear in classical systems and cannot generate nonlocal correlations [9]; for this reason, it is often dubbed as “classical entanglement”. Since its introduction by Spreeuw [10], this notion has been employed in a variety of contexts [11].

Classical entanglement has allowed to test Bell inequalities with classical wave fields. The physical significance of this violation is not linked to quantum nonlocality, but rather points to the impossibility of constructing such a beam using other beams with uncoupled degrees of freedom. However, all the experiments conducted thus far to observe this violation have involved only discrete variables, such as spin and beam path of single neutrons [12], polarization and transverse modes of a laser beam [13–17], different transverse modes propagating in multimode waveguides [18], polarization of two classical fields with different frequencies [19], orbital angular momentum [20, 21], and polarization and spatial parity [22].

In this paper, we continue the analysis of this classical entanglement by focusing on the simple but engaging example of vortex beams. To this end, in Sec. II we revisit a decomposition of Laguerre-Gauss (LG) beams in the Hermite-Gauss (HG) basis that can be rightly interpreted as a Schmidt decomposition. This immediately suggests that many ideas ensuing from the quantum world may be applicable to these beams as well. In particular, in Sec. III we address the inseparability of the LG modes using a CHSH violation that we quantify in terms of the associated Wigner function. As this distribution can be understood as a measure of the displaced parity, in Sec. IV we discuss an experimental realization which nicely agrees with the theoretical predictions. Finally, our conclusions are summarized in Sec. V.

II. OPTICAL VORTICES AND SCHMIDT DECOMPOSITION

It is well known that the beam propagation along the z direction of a monochromatic scalar field of frequency ω ; i.e., $E(\mathbf{r},t) = \mathcal{E}(\mathbf{r})\exp[-i(\omega t - kz)]$, is governed by the paraxial wave equation

$$\frac{\partial \mathcal{E}}{\partial z} = -\frac{\lambda}{2} \left(\frac{\partial^2}{\partial x^2} + \frac{\partial^2}{\partial y^2} \right) \mathcal{E}, \quad (2.1)$$

with $\lambda = \lambda/2\pi$ and λ is the wavelength. Equation (2.1) is formally identical to the Schrödinger equation for a free particle in two dimensions, with the obvious identifications $t \mapsto z$, $\psi \mapsto \mathcal{E}$, and $\hbar \mapsto \lambda$.

Any optical beam can be thus expressed as a superposition of fundamental solutions of Eq. (2.1). In Cartesian coordinates, a natural orthonormal set is given by the Hermite-Gauss (HG) modes:

$$\begin{aligned} HG_{mn}(x,y) = & \sqrt{\frac{2}{\pi n!m!2^{n+m}}} \left(\frac{1}{w} \right) H_m \left(\frac{\sqrt{2}x}{w} \right) H_n \left(\frac{\sqrt{2}y}{w} \right) \\ & \times \exp \left(-\frac{x^2+y^2}{w^2} \right), \end{aligned} \quad (2.2)$$

where w is the beam waist, and H_m are the Hermite polynomials. Note that we are restricting ourselves to the plane $z = 0$, since we are not interested here in the evolution.

For cylindrical symmetry, it is convenient to use the set of Laguerre-Gauss (LG) modes, which contain optical vortices with topological singularities; they read

$$\begin{aligned} \text{LG}_{mn}(r, \varphi) &= \sqrt{\frac{2}{\pi m! n!}} \min(m, n)! (-1)^{\min(m, n)} \left(\frac{1}{w}\right) \\ &\times \left(\frac{\sqrt{2}r}{w}\right)^{|m-n|} L_{\min(m, n)}^{|m-n|} \left(\frac{2r^2}{w^2}\right) \exp\left(-\frac{r^2}{w^2}\right) \exp[i(m-n)\varphi], \end{aligned} \quad (2.3)$$

where $L_p^{|\ell|}(x)$ are the generalized Laguerre polynomials. A word of caution seems to be in order: usually, these modes are presented in terms of two different indices: the azimuthal mode index $\ell = m - n$, which is a topological charge giving the number of 2π -phase cycles around the mode circumference, and $p = \min(m, n)$ is the radial mode index, which is related to the number of radial nodes [23]. However, the form (2.3) will be advantageous in what follows.

The crucial observation is that the LG modes can be represented as superpositions of HG modes, and viceversa. This can be compactly written down as [24]

$$\text{LG}_{mn}(\rho, \varphi) = \sum_{k=0}^{m+n} B_{mn}^k \text{HG}_{m+n-k, k}(x, y) \quad (2.4)$$

where the coefficients are

$$B_{mn}^k = \sqrt{\frac{k!(m+n-k)!}{m!n!2^{n+m}}} \frac{(-i)^k}{k!} \frac{d^k}{dt^k} [(1-t)^m (1+t)^n]|_{t=0}. \quad (2.5)$$

This looks exactly the same as a Schmidt decomposition for a bipartite quantum system. It is nothing but a particular way of expressing a vector in the tensor product of two inner product spaces [25]. Alternatively, it can be seen as another form of the singular-value decomposition [26], which identifies the maximal correlation directly. In quantum information, the Schmidt coefficients B_{mn}^k convey complete information of the entanglement [27]. Here, we intend to assess entanglement in LG beams via the violation of suitably formulated Bell inequalities.

III. CHSH VIOLATION FOR LAGUERRE-GAUSS MODES

The traditional form of the CHSH inequality applies to dichotomic discrete variables. For continuous variables, the sensible formulation is in terms of the Wigner function, which for a classical beam reads

$$W(\mathbf{x}, \mathbf{p}) = \frac{1}{\lambda^2 \pi^2} \int d^2 \mathbf{x}' e^{2i\mathbf{p} \cdot \mathbf{x}'/\lambda} \langle E^*(\mathbf{x} - \mathbf{x}') E(\mathbf{x} + \mathbf{x}') \rangle, \quad (3.1)$$

the angular brackets denoting statistical average. Although originally introduced to represent quantum mechanical phenomena in phase space [28], the Wigner distribution was established in optics [29] to relate partial coherence with radiometry. Since then, a great number of applications of this

function have been reported [30–34]. Note that W has the dimensions of an intensity and it yields a description displaying both the position and the momentum (which in the paraxial approximation has the significance of a scaled angular coordinate) of the intensity of the wave field: in fact, one easily proves that

$$\begin{aligned} \int W(\mathbf{x}, \mathbf{p}) d\mathbf{p} &= I(\mathbf{x}) \equiv \langle E^*(\mathbf{x}) E(\mathbf{x}) \rangle, \\ \frac{1}{\lambda^2 \pi^2} \int W(\mathbf{x}, \mathbf{p}) d\mathbf{x} &= I(\mathbf{p}) \equiv \langle E^*(\mathbf{p}) E(\mathbf{p}) \rangle, \end{aligned} \quad (3.2)$$

with

$$E(\mathbf{p}) = \frac{1}{\lambda^2 \pi^2} \int E(\mathbf{x}) \exp(i\mathbf{p} \cdot \mathbf{x}/\lambda) d\mathbf{x}. \quad (3.3)$$

Thus, the marginals of the Wigner function are the intensity distributions in \mathbf{x} or \mathbf{p} space, respectively.

The CHSH inequality can now be stated in terms of the Wigner function as [35]

$$B = \frac{\pi^2}{4} |W(\alpha, \beta) + W(\alpha, \beta') + W(\alpha', \beta) - W(\alpha', \beta')| < 2, \quad (3.4)$$

where $\alpha = (x, p_x)/\sqrt{2}$ and $\beta = (y, p_y)/\sqrt{2}$. This also follows from the work of Gisin [36], who formulated a Bell inequality for the set of observables with the property $\hat{O}^2 = \mathbb{1}$: as we shall see, the Wigner function appears as the average value of the parity, whose square is unity. Reference [21] presents a detailed study of the violations of (3.4).

For the state LG_{mn} , the normalized Wigner function can be written as [37]

$$\begin{aligned} W_{mn}^{\text{LG}}(X, P_X; Y, P_Y) &= \frac{(-1)^{m+n}}{\pi^2} \exp(-4Q_0) \\ &\times L_m[4(Q_0 + Q_2)] L_n[4(Q_0 - Q_2)], \end{aligned} \quad (3.5)$$

where

$$Q_0 = \frac{1}{4}(X^2 + Y^2 + P_X^2 + P_Y^2), \quad Q_2 = \frac{1}{2}(XP_Y - YP_X), \quad (3.6)$$

and we have rescaled the variables as $x \mapsto (w/\sqrt{2})X$ and $p_x \mapsto (\sqrt{2}\lambda/w)P_X$ (and analogously for the y axis). Let us first look at the simple case of the mode LG_{10} , which reduces to

$$\begin{aligned} W_{10}^{\text{LG}}(X, P_X; Y, P_Y) &= \frac{1}{\pi^2} \exp(-P_X^2 - P_Y^2 - X^2 - Y^2) \\ &\times [(P_X - Y)^2 + (P_Y + X)^2 - 1]. \end{aligned} \quad (3.7)$$

The two measurement settings on one side are chosen to be $\alpha = (X = 0, P_X = 0)$ and $\alpha' = (X' = X, P'_X = 0)$, and the corresponding settings on the other side are $\beta = (Y = 0, P_Y = 0)$ and $\beta' = (Y' = 0, P'_Y = P_Y)$ [38], for which the Bell sum is

$$\begin{aligned} B &= e^{-P_Y^2} (P_Y^2 - 1) + e^{-X^2} (X^2 - 1) \\ &- e^{-(P_Y^2 + X^2)} [(P_Y + X)^2 - 1] - 1. \end{aligned} \quad (3.8)$$

Upon maximization with respect to X and P_Y , we obtain the maximum Bell violation, $|B_{\max}| \simeq 2.17$, which happens for the choices $X \simeq 0.45$, $P_Y \simeq 0.45$ [21]. For comparison, note that the maximum Bell violation in quantum mechanics through the Wigner function for the two-mode squeezed vacuum state using similar settings is given by $|B_{\max}^{\text{QM}}| \simeq 2.19$ [35].

The Bell violation may be further optimized by a more general choice of settings than those used here. For example, maximizing it with respect to the parameters $\alpha = (X, P_X)$, $\alpha' = (X', P'_X)$, $\beta = (Y, P_Y)$, $\beta' = (Y', P'_Y)$, one obtains the absolute maximum Bell violation, $|B_{\max}| = 2.24$ and occurs for the choices $X \simeq -0.07$, $P_X \simeq 0.05$, $X' \simeq 0.4$, $P'_X \simeq -0.26$, $Y \simeq -0.05$, $P_Y \simeq -0.07$, $Y' \simeq 0.26$, $P'_Y \simeq 0.4$. The violation also increases with higher orbital angular momentum. This increase with n is analogous to the enhancement of nonlocality in quantum mechanics for many-particle Greenberger-Horne-Zeilinger states [39].

IV. EXPERIMENTAL RESULTS

We have carried a direct measurement of the Bell sums for optical beams with different amount of nonlocal correlations. To understand the measurement, we recall that the Wigner function in quantum optics is often regarded as the average of the displaced parity operator [40]. At the classical level, we can consider the field amplitudes $\mathcal{E}(X, Y)$ as vectors in the Hilbert space of complex-valued functions that are square integrable over a transverse plane. In this space we define linear Hermitian operators

$$\hat{X} : \mathcal{E}(X, Y) \mapsto X \mathcal{E}(X, Y), \quad \hat{P}_x : \mathcal{E}(X, Y) \mapsto -i \frac{\partial}{\partial X} \mathcal{E}(X, Y), \quad (4.1)$$

and analogous ones for the Y variable. Formally, these operators satisfy the canonical commutation relations $[\hat{X}, \hat{P}_X] = [\hat{Y}, \hat{P}_Y] = i$. Therefore, the unitary parity operator is

$$\hat{\Pi}_X \hat{X} \hat{\Pi}_X = -\hat{X}, \quad \hat{\Pi}_X \hat{P}_X \hat{\Pi}_X = -\hat{P}_X, \quad (4.2)$$

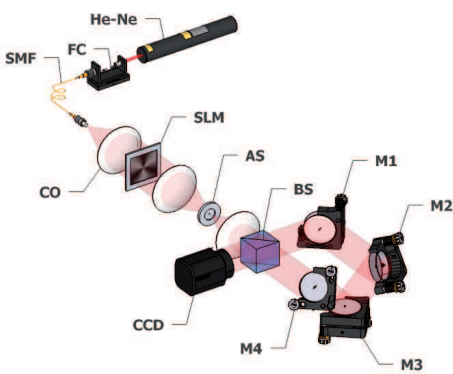


FIG. 1. (Color online) Scheme of the Bell measurement. The abbreviations are as follows: He-Ne: laser source, FC: fiber coupler, SMF: single mode fiber, CO: collimation optics, SLM: spatial light modulator, AS: aperture stop, BS: beam splitter, M1-M4: mirrors, CCD: camera

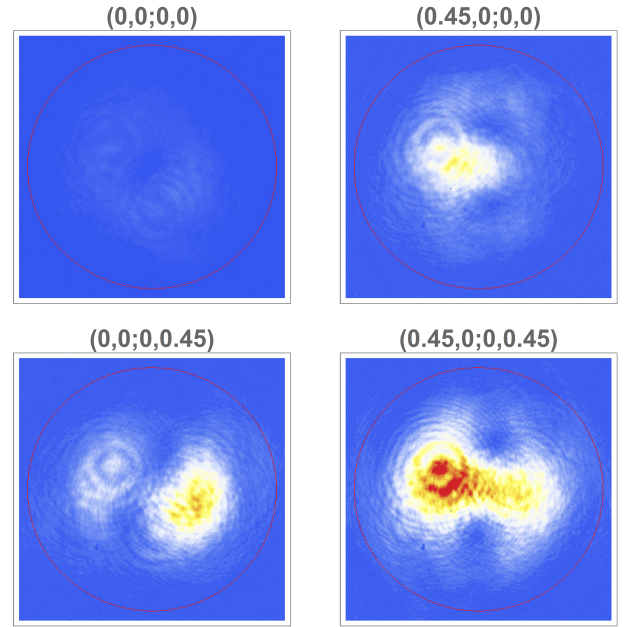


FIG. 2. (Color online) Snapshots of the CCD camera for the state LG_{10} at the four settings $(X, P_X; Y, P_Y)$ indicated. The scans are normalized to the peak intensity among the measurements and the area of interest for the intensity integration is marked by a red circle.

and changes $\mathcal{E}(X, Y)$ into $\mathcal{E}(-X, Y)$. The displacement operators are

$$\hat{D}(X, P_X) = \exp[i(P_X \hat{X} - X \hat{P}_X)]. \quad (4.3)$$

Indeed, with these notations we have

$$W(X, P_x; Y, P_y) = \frac{4}{\pi^2} \langle \hat{D}(X, P_x) \hat{\Pi}_X \hat{D}^\dagger(X, P_x) \hat{D}(Y, P_y) \hat{\Pi}_Y \hat{D}^\dagger(Y, P_y) \rangle. \quad (4.4)$$

Parity measurement can be, in turn, realized by a common-path interferometer with a Dove prism inserted into the optical path [41]. In our setup, sketched in Fig. 1, the prism was substituted with an equivalent four-mirror Sagnac arrangement [42]. The two copies of the input signal obtained after the input beam splitter are transformed by the mirrors so as to make one copy spatially inverted with respect to the other, prior to combining the beams together. The resulting interference pattern is detected by a CCD camera: Figure 2 shows snapshots of the camera for the state LG_{10} at the four settings indicated. The total intensity witnessing parity of the measured beam is computed by spatial integration and this is proportional to the desired Wigner distribution sample after normalization to the overall intensity.

The target signal beams were prepared with digital holograms created by a spatial light modulator (SLM), which modulated a collimated output of a single mode fiber coupled to a He-Ne laser. We also included a 4f-system, with an aperture stop, to filter the unwanted diffraction orders produced by the SLM. To allow for a better flexibility, all the necessary shifts

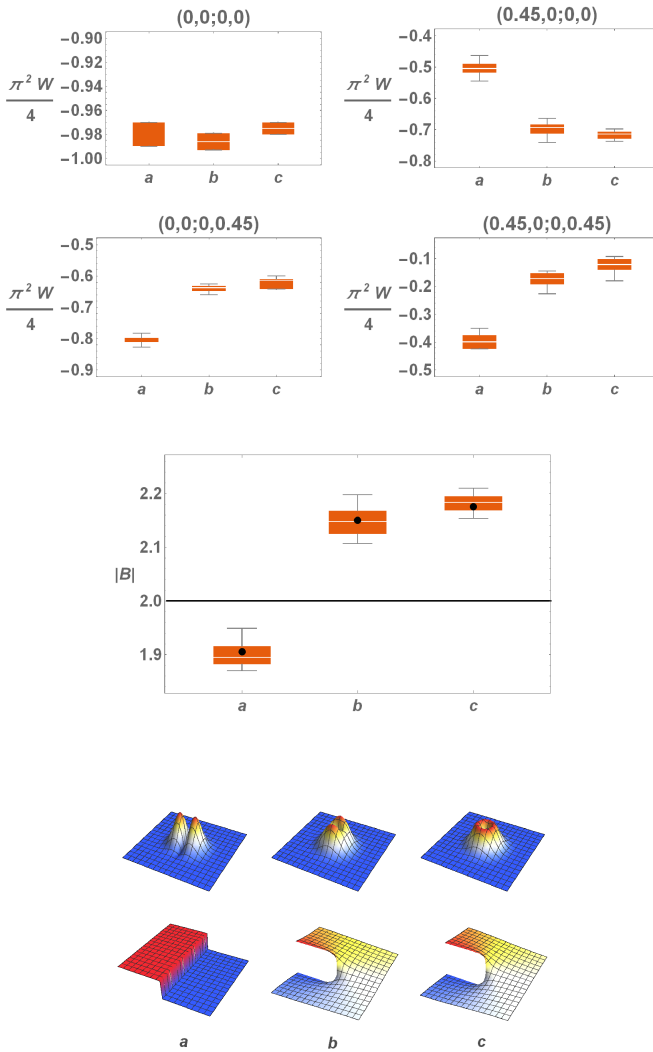


FIG. 3. (Color online) Experimental results for three different optical beams: a) HG_{10} , b) $0.4\text{HG}_{10} + i0.6\text{HG}_{01}$, and c) LG_{10} . At the top, we plot $\frac{\pi^2}{4}W(X, P_X; Y, P_Y)$ at the values $(X, P_X; Y, P_Y)$ indicated for each one. The next plot shows the measured Bell sums, all reported with 75% and 25% quartile (orange boxes) and the minimal and maximal measured values (error bars). The theoretical values $(-1.91, -2.15, -2.17)$ are the dots and the black bar is at $|B| = 2$, which delimits the classically entangled states. The theoretical amplitude (top) and phase (bottom) distributions of the measured beams are plotted below the chart.

in the X , Y , P_X , and P_Y variables were incorporated into the SLM, so that each Bell measurement was associated with a separate hologram.

The measured beams were coherent superpositions of Hermite-Gaussian beams in the form $a\text{HG}_{10} + ib\text{HG}_{01}$ with $\{a = 1, b = 0\}$, $\{a = 0.4, b = 0.6\}$ and $\{a = 0.5, b = 0.5\}$, respectively. The first and the third are thus a pure Hermite-Gaussian beam and a pure Laguerre-Gaussian vortex beam, respectively. For all the beams we used the settings $X \simeq$

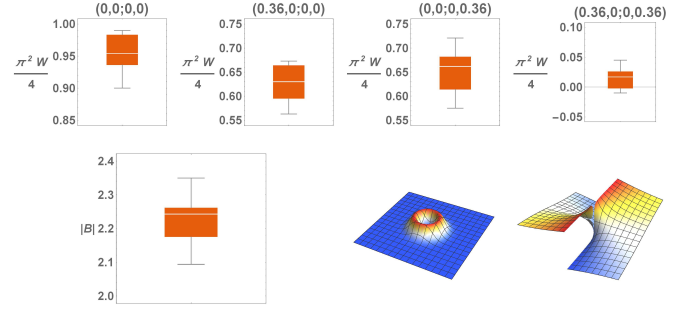


FIG. 4. (Color online) Experimental results for the beam LG_{20} , as presented in Fig. 3. The values of $(X, P_X; Y, P_Y)$ are also indicated. The Bell sum variation is significantly larger than in the case of LG_{10} . The plots on the right bottom panel are the amplitude and phase of LG_{20} .

0.0, $P_X \simeq 0.0$, $X' \simeq -0.45$, $P'_X \simeq 0.0$, $Y \simeq 0.0$, $P_Y \simeq 0.0$, $Y' \simeq 0.0$, $P'_Y \simeq -0.45$ for the evaluation of the Bell sums. The theoretical values of the Bell sums for these are $(-1.91, -2.15, -2.17)$, respectively.

Each measurement was repeated many times with slightly different readings, due to laser intensity instabilities and CCD noise. These effects manifest as measurement errors, which can be estimated from the sample statistics. As the parity measurement requires to normalize the total measured intensity of the interference pattern with respect to the input beam intensity, a separate reading of the input beam intensity was performed. For each optical beam, the mean value of the Bell sum is reported. The results are summarized in Fig. 3. The Bell correlations grow with the coupling between the basis HG_{10} and HG_{01} modes, with statistically significant violation of CHSH inequality by the second and third beams, as theoretically predicted.

We also show the measured values of the Wigner function. For both, HG_{10} and LG_{10} modes, the values of $\pi^2W(0, 0; 0, 0)$ are quite close to -1 . For classical beams, ours is one of the few measurements on the negativity of the Wigner function, though it has to be anticipated from the corresponding results in quantum optics [43]. We note that very early, March and Wolf [44] had constructed an example of a classical source which exhibited negative Wigner function.

Finally, we have checked the violation of CHSH inequality for the beam LG_{20} . A beam with higher topological charge is more sensitive to setup imperfections, hence the Bell sum variation is significantly larger than in the case of LG_{10} . On the other hand, as shown in Fig. 4, the increasing of the Bell sum for higher orbital angular momentum is clearly demonstrated: the theoretical value for LG_{20} is -2.24 , which agrees pretty well with the experimental results. [45]. Note that the Wigner function at the origin for the LG_{20} beam is positive, as expected.

V. CONCLUDING REMARKS

In short, we have presented an experimental study of nonlocal correlations in classical beams with topological singularities [21]. These correlations between modes are manifested through the violation of a CHSH inequality, which we have detected via direct parity measurements. Such a violation is shown to increase with the value of orbital angular momentum of the beam. As a byproduct of our measurements, we obtain negativity of the Wigner function at certain points in phase space for the HG₁₀ and LG₁₀ beams. Note that this has implications for similar studies with electron beams, for which vortices have been reported [46, 47].

Though entanglement here does not bear any paradoxical meaning, such as “spooky action on the distance”, it still represents a potential resource for classical signal processing. It might be expected that future applications of quantum information processing can be tailored in terms of classical light:

the research presented in this work explores one of those options.

Furthermore, our results are relevant not only for a correct understanding of “classical entanglement”, but also for bringing out different statistical features of the optical beams, since it provides an alternative paradigm to the well developed optical coherence theory.

ACKNOWLEDGMENTS

We acknowledge illuminating discussions with Gerd Leuchs, Elisabeth Giacobino, and Andrea Aiello. This work was supported by the Grant Agency of the Czech Republic (Grant 15-031945), the European Social Fund and the State Budget of the Czech Republic POSTUP II (Grant CZ.1.07/2.3.00/30.0041), the IGA of the Palacký University (Grant PrF-2015-002), the Spanish MINECO (Grant FIS2011-26786), and UCM-Banco Santander Program (Grant GR3/14).

[1] E. Schrödinger, “Discussion of probability relations between separated systems,” *Math. Proc. Cambridge Philos. Soc.* **31**, 555–563 (1935).

[2] A. Einstein, B. Podolsky, and N. Rosen, “Can quantum-mechanical description of physical reality be considered complete?” *Phys. Rev.* **47**, 777–780 (1935).

[3] R. Horodecki, P. Horodecki, M. Horodecki, and K. Horodecki, “Quantum entanglement,” *Rev. Mod. Phys.* **81**, 865–942 (2009).

[4] J. Bell, “On the Einstein Podolsky Rosen paradox,” *Physics* **1**, 195–200 (1964).

[5] J. F. Clauser, M. A. Horne, A. Shimony, and R. A. Holt, “Proposed experiment to test local hidden-variable theories,” *Phys. Rev. Lett.* **23**, 880–884 (1969).

[6] N. Brunner, D. Cavalcanti, S. Pironio, V. Scarani, and S. Wehner, “Bell nonlocality,” *Rev. Mod. Phys.* **86**, 419–478 (2014).

[7] R. F. Werner and M. M. Wolf, “Bell inequalities and entanglement,” *Quant. Inform. Comput.* **1**, 1–25 (2001).

[8] F. Töppel, A. Aiello, C. Marquardt, E. Giacobino, and G. Leuchs, “Classical entanglement in polarization metrology,” *New J. Phys.* **16**, 073019 (2014).

[9] N. Brunner, N. Gisin, and V. Scarani, “Entanglement and nonlocality are different resources,” *New J. Phys.* **7**, 88 (2005).

[10] R. J. C. Spreeuw, “A classical analogy of entanglement,” *Found. Phys.* **28**, 361–374 (1998).

[11] P. Ghose and A. Mukherjee, “Entanglement in classical optics,” *Rev. Theor. Sci.* **2**, 1–14 (2014).

[12] Y. Hasegawa, R. Loidl, G. Badurek, M. Baron, and H. Rauch, “Violation of a Bell-like inequality in single-neutron interferometry,” *Nature* **425**, 45–48 (2003).

[13] C. E. R. Souza, J. A. O. Huguenin, P. Milman, and A. Z. Khouri, “Topological phase for spin-orbit transformations on a laser beam,” *Phys. Rev. Lett.* **99**, 160401 (2007).

[14] B. N. Simon, S. Simon, F. Gori, M. Santarsiero, R. Borghi, N. Mukunda, and R. Simon, “Nonquantum entanglement resolves a basic issue in polarization optics,” *Phys. Rev. Lett.* **104**, 023901 (2010).

[15] X.-F. Qian and J. H. Eberly, “Entanglement and classical polarization states,” *Opt. Lett.* **36**, 4110–4112 (2011).

[16] C. Gabriel, A. Aiello, W. Zhong, T. G. Euser, N. Y. Joly, P. Banzer, M. Förtsch, D. Elser, U. L. Andersen, Ch. Marquardt, P. St. J. Russell, and G. Leuchs, “Entangling different degrees of freedom by quadrature squeezing cylindrically polarized modes,” *Phys. Rev. Lett.* **106**, 060502 (2011).

[17] X. F. Qian, B. Little, J. C. Howell, and J. H. Eberly, “Violation of Bell’s inequalities with classical Shimony-Wolf states: Theory and experiment,” *arXiv:1406.3338*.

[18] J. Fu, Z. Si, S. Tang, and J. Deng, “Classical simulation of quantum entanglement using optical transverse modes in multimode waveguides,” *Phys. Rev. A* **70**, 042313 (2004).

[19] K. F. Lee and J. E. Thomas, “Experimental simulation of two-particle quantum entanglement using classical fields,” *Phys. Rev. Lett.* **88**, 097902 (2002).

[20] S. K. Goyal, F. S. Roux, A. Forbes, and T. Konrad, “Implementing quantum walks using orbital angular momentum of classical light,” *Phys. Rev. Lett.* **110**, 263602 (2013).

[21] P. Chowdhury, A. S. Majumdar, and G. S. Agarwal, “Nonlocal continuous-variable correlations and violation of Bell’s inequality for light beams with topological singularities,” *Phys. Rev. A* **88**, 013830 (2013).

[22] K. H. Kagalwala, G. Di Giuseppe, A. F. Abouraddy, and B. E. A. Saleh, “Bell’s measure in classical optical coherence,” *Nat. Photon.* **7**, 72–78 (2013).

[23] E. Karimi, R. W. Boyd, P. de la Hoz, H. de Guise, J. Řeháček, Z. Hradil, A. Aiello, G. Leuchs, and L. L. Sánchez-Soto, “Radial quantum number of Laguerre-Gauss modes,” *Phys. Rev. A* **89**, 063813 (2014).

[24] M. W. Beijersbergen, L. Allen, H.E.L.O. van der Veen, and J. P. Woerdman, “Astigmatic laser mode converters and transfer of orbital angular momentum,” *Opt. Commun.* **96**, 123–132 (1993).

[25] A. Peres, *Quantum Theory: Concepts and Methods* (Kluwer, Dordrecht, 1993).

[26] G. W. Stewart, “On the early history of the singular value decomposition,” *SIAM Rev.* **35**, 551–566 (1993).

[27] G. S. Agarwal and J. Banerji, “Spatial coherence and information entropy in optical vortex fields,” *Opt. Lett.* **27**, 800–802 (2002).

[28] E. Wigner, “On the quantum correction for thermodynamic equilibrium,” *Phys. Rev.* **40**, 749–759 (1932).

[29] A. Walther, “Radiometry and coherence,” *J. Opt. Soc. Am.* **58**, 1256–1259 (1968).

[30] M. J. Bastiaans, “Phase-space optics: fundamentals and applications,” (McGraw-Hill, New York, 2009) Chap. Wigner distribution in optics, pp. 1–44.

[31] Lorenzo Galleani and Leon Cohen, “The wigner distribution for classical systems,” *Phys. Lett. A* **302**, 149–155 (2002).

[32] D. Dragoman, “The wigner distribution function in optics and optoelectronics,” in *Progress in Optics*, Vol. 37, edited by E. Wolf (Elsevier, Amsterdam, 1997).

[33] W. Mecklenbraüker and F. Hlawatsch, *The Wigner Distribution: Theory and Applications in Signal Processing* (Elsevier, Amsterdam, 1997).

[34] Miguel A. Alonso, “Wigner functions in optics: describing beams as ray bundles and pulses as particle ensembles,” *Adv. Opt. Photon.* **3**, 272–365 (2011).

[35] K. Banaszek and K. Wódkiewicz, “Testing quantum nonlocality in phase space,” *Phys. Rev. Lett.* **82**, 2009–2013 (1999).

[36] N. Gisin, “Bell’s inequality holds for all non-product states,” *Phys. Lett. A* **154**, 201–202 (1991).

[37] R. Simon and G. S. Agarwal, “Wigner representation of laguerre–gaussian beams,” *Opt. Lett.* **25**, 1313–1315 (2000).

[38] L. Zhang, A. B. U’ren, R. Erdmann, K. A. O’Donnell, C. Silberhorn, K. Banaszek, and I. A. Walmsley, “Generation of highly entangled photon pairs for continuous variable Bell inequality violation,” *J. Mod. Opt.* **54**, 707–719 (2007).

[39] N. D. Mermin, “Extreme quantum entanglement in a superposition of macroscopically distinct states,” *Phys. Rev. Lett.* **65**, 1838–1840 (1990).

[40] A. Royer, “Wigner function as the expectation value of a parity operator,” *Phys. Rev. A* **15**, 449–450 (1977).

[41] E. Mukamel, K. Banaszek, I. A. Walmsley, and C. Dorner, “Direct measurement of the spatial Wigner function with area-integrated detection,” *Opt. Lett.* **28**, 1317–1319 (2003).

[42] B. J. Smith, B. Killett, M. G. Raymer, I. A. Walmsley, and K. Banaszek, “Measurement of the transverse spatial quantum state of light at the single-photon level,” *Opt. Lett.* **30**, 3365–3367 (2005).

[43] W. Schleich, *Quantum Optics in Phase Space* (VCH-Wiley, Berlin, 2000).

[44] E. W. Marchand and E. Wolf, “Radiometry with sources of any state of coherence,” *J. Opt. Soc. Am.* **64**, 1219–1226 (1974).

[45] A study of the Bell violations for LG beams is also presented by S. Prabhakar, S. G. Reddy, A. A. Chithrabhanu, P. G. K. Samantha, and R. P. Singh, arxiv:1406.6239, although the authors does not employ parity measurements, but Fourier transform.

[46] J. Verbeeck, H. Tian, and P. Schattschneider, “Production and application of electron vortex beams,” *Nature* **467**, 301–304 (2010).

[47] B. J. McMorran, A. Agrawal, I. M. Anderson, A. A. Herzing, z H. J. Lezec, J. J. McClelland, and J. Unguris, “Electron vortex beams with high quanta of orbital angular momentum,” *Science* **331**, 192–195 (2011).